Synthesis, Structural Evolution, and Theoretical and Physical Studies of the Novel Compounds $M_2Mo_9S_{11}$ (M = K, Rb) and Related Metastable Materials $Cu_xK_{1.8}Mo_9S_{11}$ (x = 0 or 2) Containing Bioctahedral Mo_9 Clusters

Soazig Picard, Jean-François Halet, Patrick Gougeon,* and Michel Potel

Université de Rennes 1, Laboratoire de Chimie du Solide et Inorganique Moléculaire, UMR 6511, Avenue du Général Leclerc, 35042 Rennes Cedex, France

Received April 1, 1999

The new isostructural $K_2Mo_9S_{11}$ and $Rb_2Mo_9S_{11}$ phases were prepared by solid-state reaction at 1500 °C in a sealed molybdenum crucible. Both compounds crystallize in the trigonal space group (SG) $R\bar{3}c$, $Z = 6$, a = 9.271(1) Å, c = 35.985(9) Å and a = 9.356(2) Å, c = 35.935(9) Å for the K and Rb compounds, respectively, in the hexagonal setting. Their crystal structures were determined from single-crystal X-ray diffraction data and consist of interconnected Mo_9S_{11} units forming an original and unprecedented three-dimensional framework. Extended Hückel tight-binding (EHTB) calculations carried out on $K_2Mo_9S_{11}$ indicate that such compounds are electron-deficient and may be reduced without altering the arrangement of the Mo_9S_{11} units. This was verified by the insertion of copper into $K_2Mo_9S_{11}$ by topotactic oxydo-reduction reaction, which leads to the new metastable $Cu_2K_{1.8}Mo_9S_{11}$ compound (SG $R\bar{3}c$, a = 9.4215(4) Å, c = 35.444(2) Å, $Z = 6$). The potassium nonstoichiometry of this quaternary phase was confirmed by deintercalation of the copper in a HCl 12 M solution at 80 °C, leading to the $K_{1.8}Mo_9S_{11}$ phase (SG $R\bar{3}c$, a = 9.2801(8) Å, c = 35.833(7) Å, $Z = 6$). The X-ray single-crystal structures of $K_{1.8}Mo_9S_{11}$ and $Cu_2K_{1.8}Mo_9S_{11}$ are also described. Electrical resistivity measurements carried out on single crystals of $K_2Mo_9S_{11}$ and $Cu_2K_{1.8}Mo_9S_{11}$ indicate that the former is metallic whereas the latter is semiconducting, as expected from EHTB calculations. Magnetic and electrical resistivity measurements performed on $K_{1.8}Mo_9S_{11}$ reveal a superconducting behavior below 4.5 K.

Introduction

Over the last three decades, a large number of ternary and quaternary reduced molydenum chalcogenides with metal clusters of diverse sizes and geometries have been synthesized by solid-state reaction at high temperature (1200−1800 °C). Compounds containing octahedral Mo_6 clusters[1] are the most abundant and present interesting physical properties.[2,3] Molybdenum clusters with nuclearity higher than six such as Mo_9,[4] Mo_{12},[5] Mo_{15},[6] Mo_{18},[7] Mo_{21},[8] Mo_{24},[9] Mo_{30},[9] and Mo_{36}[10] result from the uniaxial trans-face sharing of Mo_6 octahedra. Among the latter, the first condensed cluster, which was observed 20 years ago, is the bioctahedral Mo_9 cluster which was found to coexist in equal proportion with the Mo_6 cluster in the $M_2Mo_{15}Se_{19}$ (M = K, In, Ba, Tl),[11] $K_2Mo_{15}S_{19}$,[11] and $In_3Mo_{15}Se_{19}$[12] compounds. These Mo_6−Mo_9 cluster compounds are generally superconducting materials with critical temperature (T_c) ranging between 1.2 and 4.3 K. In addition, $In_3Mo_{15}Se_{19}$[13] exhibits a critical field with an initial slope as high as 7.8 T/K at T_c. Recent band structure calculations on $Rb_2Mo_{15}S_{19}$[14] showed that the Mo_6 and Mo_9 units are hypoelectronic species with 20 and 34 metallic electrons (MEs), the closed-shell configuration corresponding to 24 and 36 electrons, respectively. Subsequently, the Mo_9 cluster was found alone in $Ag_{3.6}Mo_9Se_{11}$[4] (space group (SG) *Cmcm*) and $Ag_{2.3}CsMo_9Se_{11}$[9] (SG $P6_3/m$). Both compounds are semiconducting because of the closed-shell configuration of the Mo_9 cluster with roughly 36 MEs per Mo_9 cluster. In the case of $Ag_{3.6}Mo_9Se_{11}$, the topotactic silver deintercalation leads to the metastable binary *o*-Mo_9Se_{11}[15] with 32 MEs per Mo_9 cluster, which exhibits a metallic behavior with a superconducting transition at 5.5 K. In addition, it is interesting to note that a similar geometrical metallic core is also found in molecular chemistry with rhenium in $[Re_9Se_{11}Br_6][PPh_4]_2$,[16] cobalt in $Co_9Se_{11}(PPh_3)_6$,[17] and nickel in $[Ni_9S_9(PEt_3)_6]^{2+}$.[18]

(1) Chevrel, R.; Sergent, M. In *Superconducting in Ternary Compounds*; Fischer, Ø., Maple, M. B., Eds.; Springer-Verlag: Berlin, Heidelberg, New York, 1982; Part I.
(2) Fischer, Ø. *Appl. Phys.* **1978**, *16*, 1.
(3) Maple, M. B.; Fischer, Ø. In *Superconducting in Ternary Compounds*; Fischer, Ø., Maple, M. B., Eds.; Springer-Verlag: Berlin, 1982; Parts I and II.
(4) Gougeon, P.; Padiou, J.; Le Marouille, J.-Y.; Potel, M.; Sergent, M. *J. Solid State Chem.* **1984**, *51*, 226.
(5) (a) Gougeon, P.; Potel, M.; Padiou, J.; Sergent, M. *Mater. Res. Bull.* **1987**, *22*, 1087. (b) Gautier, R.; Picard, S.; Gougeon, P.; Potel, M. *Mater. Res. Bull.* **1999**, *34*, 93.
(6) (a) Gougeon, P.; Potel, M.; Sergent, M. *Acta Crystallogr.* **1989**, *C45*, 182. (b) Gougeon, P.; Potel, M.; Sergent, M. *Acta Crystallogr.* **1989**, *C45*, 1413.
(7) Gougeon, P.; Potel, M.; Padiou, J.; Sergent, M. *Mater. Res. Bull.* **1988**, *23*, 453.
(8) Picard, S.; Gougeon, P.; Potel, M. *Acta Crystallogr.* **1997**, *C53*, 1519.
(9) Gougeon, P. Thesis, Université de Rennes 1, 1984.
(10) Picard, S.; Gougeon, P.; Potel, M. *Angew. Chem., Int. Ed.* **1999**, *38*, 2034.
(11) (a) Chevrel, R.; Potel, M.; Sergent, M.; Decroux, M.; Fischer, Ø. *Mater. Res. Bull.* **1980**, *15*, 867. (b) Potel, M.; Chevrel, R.; Sergent, M. *Acta Crystallogr.* **1981**, *B37*, 1007.
(12) Gruttner, A.; Yvon, K.; Chevrel, R.; Potel, M.; Sergent, M.; Seeber, B. *Acta Crystallogr.* **1979**, *B35*, 285.
(13) Seeber, B.; Decroux, M.; Fisher, Ø.; Chevrel, R.; Sergent, M.; Grüttner, A. *Solid State Chem.* **1979**, *29*, 414.
(14) Picard, S.; Noel, H.; Gougeon, P.; Potel, M. First International Conference on Inorganic Materials, Versailles, France, Sept 16−19, 1998.
(15) Gougeon, P.; Potel, M.; Padiou, J.; Sergent, M.; Boulanger, C.; Lecuire, J.-M. *J. Solid State Chem.* **1984**, *218*, 226.

10.1021/ic990362b CCC: $18.00
Published on Web 09/16/1999

We present, here, the syntheses, crystal structures, and physical properties of $K_2Mo_9S_{11}$, $Rb_2Mo_9S_{11}$, $Cu_2K_{1.8}Mo_9S_{11}$, and $K_{1.8}Mo_9S_{11}$ which crystallize in a new structural type built up with Mo_9S_{11} units. The electronic band structure of the former compound is also described and correlated to the electrical behaviors of these series of compounds.

Experimental Section

Syntheses. Starting materials used for the syntheses were MoS_2, M_2MoS_4 (M = K, Rb), and Mo, all in powder form. Before use, Mo powder (Plansee) was reduced under H_2 flowing gas at 1000 °C for 10 h to eliminate any trace of oxygen. The molybdenum disulfide was prepared by the reaction of sulfur (Fluka, 99.999%) with H_2-reduced Mo in a ratio of 2:1 in an evacuated (ca. 10^{-2} Pa of Ar residual pressure) and flame-baked sealed silica tube, heated at 800 °C for 2 days. The thiomolybdates of alkali metals were obtained by sulfuration of M_2MoO_4 (M = K, Rb), at 400 and 450 °C, respectively, for 2 days using CS_2 gas in a flowing argon carrier. Molybdates M_2MoO_4 (M = K, Rb) were synthesized by heating an equimolar ratio of MoO_3 (CERAC, 99.95%) and M_2CO_3 (M = K, Rb) (Strem Chemicals, 99%; CERAC, 99.9%, respectively) in an alumina vessel at 800 °C in air for 2 days. The purity of all starting reagents was checked by powder X-ray diffraction on an Inel curve-sensitive position detector CPS 120. Furthermore, to avoid any contamination by oxygen and moisture, the starting reagents were kept and handled in a purified argon-filled glovebox.

$K_2Mo_9S_{11}$ (1). Pure X-ray $K_2Mo_9S_{11}$ powder was synthesized by a high-temperature solid-state reaction from a stoichiometric mixture of K_2MoS_4, MoS_2, and Mo. The powders were mixed, ground together in a mortar and then cold-pressed. The pellet (ca. 3 g) was then loaded in a molybdenum crucible (depth 2.5 cm, diameter 1.5 cm) which was previously cleaned by heating at 1500 °C in a high-frequency furnace for 15 min under a dynamic vacuum of about 10^{-3} Pa and then sealed under a low argon pressure (300 hPa) using an arc welding system. The crucible was heated at a rate of 300 °C·h^{-1} to 1500 °C and held there for 6 h, then cooled at 100 °C·h^{-1} to 1000 °C, and finally furnace cooled to room temperature. The resulting product was black and air-stable and was found as a pure phase on the basis of its X-ray powder diffraction diagram.

Single crystals of $K_2Mo_9S_{11}$ of quality and size suitable for X-ray diffraction and resistivity measurements were obtained with an overall composition richer in K_2S (5%). The final product was a mixture of $K_2Mo_9S_{11}$ and $K_2Mo_{15}S_{19}$ crystals which could be separated manually due to their different morphologies.

$Rb_2Mo_9S_{11}$ (2). The same preparative method was used for $Rb_2Mo_9S_{11}$ to obtain microcrystallized powder and single crystals. However, $Rb_2Mo_9S_{11}$ was only synthesized from overall compositions richer in Rb_2S (>5%) than the stoichiometric one. Indeed, the formal starting composition $Rb_2Mo_9S_{11}$ leads to a mixture of $Rb_2Mo_{15}S_{19}$[14] and $Rb_6Mo_{27}S_{31}$[14] with no trace of the $Rb_2Mo_9S_{11}$ compound. But, whatever starting compositions were used, $Rb_2Mo_9S_{11}$ was never obtained as a single phase.

$Cu_2K_{1.8}Mo_9S_{11}$(3). The copper-intercalated compound $Cu_2K_{1.8}Mo_9S_{11}$ was synthesized by topotactic oxydo-reduction reaction between previously prepared $K_2Mo_9S_{11}$ crystals and an excess of Cu powder in a molar ratio of 1:10. The mixture was heated at 750 °C for 300 h in an evacuated silica tube which was finally slowly cooled to room temperature at 10 °C·h^{-1}. This compound, which is only obtainable by this low-temperature route, decomposes mainly into $Cu_xMo_6S_8$ and $K_2Mo_6S_6$ above 800 °C.

$K_{1.8}Mo_9S_{11}$(4). The $K_{1.8}Mo_9S_{11}$ compound was prepared by washing previously intercalated $Cu_2K_{1.8}Mo_9S_{11}$ in a 12 M hydrochloric acid solution at 80 °C for 72 h, which effectively removed all the copper.

Single-Crystal X-ray Studies. Four black single crystals of $K_2Mo_9S_{11}$ (**1**), $Rb_2Mo_9S_{11}$ (**2**), $Cu_2K_{1.8}Mo_9S_{11}$ (**3**), and $K_{1.8}Mo_9S_{11}$ (**4**) with rhombohedral or truncated octahedral shapes and approximate dimensions 0.08 × 0.07 × 0.04, 0.06 × 0.06 × 0.08, 0.09 × 0.07 × 0.06, and 0.05 × 0.05 × 0.05 mm^3, respectively, were selected and mounted on glass fibers. They were investigated by the $\omega-2\theta$ scan method in the 4−80° 2θ range at room temperature on an automatic X-ray Nonius CAD-4 diffractometer equipped with graphite-monochromatized MoKα radiation (λ = 0.71073 Å). Lattice parameters were obtained by least-squares refinement of the setting angles of 25 reflections. In all cases, three orientation and three intensity reference reflections were checked every 250 reflections and every hour, respectively, and showed no significant fluctuation during data collection. For the four single crystals measured, the intensities were collected in the (h,k,l) ranges 0/16,0/16,−65/+65 for **1** and **2** and 0/17,0/17,−64/+64 for **3** and **4**. The raw data were then corrected for Lorentz polarization and for absorption using the ψ-scan technique on six reflections with the aid of the XRAYACS program[19] (no absorption correction for **4**). The unscaled transmission factors were in the range 0.864−1.0 for **1**, 0.870−1.0 for **2**, and 0.936−1.0 for **3**. Systematic absences $-h + k + l \neq 3n$ and $h - h0l$, $l = 2n + 1$, were only consistent with $R3c$ and $R\bar{3}c$ space groups. Atomic scattering factors and anomalous dispersion corrections were taken from the *Table for X-ray Crystallography* (1974).

$K_2Mo_9S_{11}$ (1). The crystal structure of $K_2Mo_9S_{11}$ was solved with the direct method program SHELXS[20] in the $R\bar{3}c$ space group using the 3678 collected reflections (1650 unique reflections with $I/\sigma(I) > 2$, R_{int} = 0.0188). Full-matrix least-squares refinement using F on positional and anisotropic displacement parameters for all atoms was carried out using the JANA98 program.[21] The obverse−reverse twinning matrix [−1,0,0; 0,−1,0; 0,0,1] was introduced then in the refinement. This revealed a very low twinning ratio (1.37(7)%) that significantly improved the reliability factors, according to the Hamilton test.[22] Indeed, for the independent data having $I/\sigma(I) > 2$, the final refinement cycle converged to the values of $R(F_o)$ = 0.0186 and $R_w(F_o)$ = 0.0207 for 37 refined parameters, instead of $R(F_o)$ = 0.0198 and $R_w(F_o)$ = 0.0224 for 36 refined parameters. The maximum shift/σ ratio for all the refined parameters was less than 0.0017 and S = 2.14. The secondary extinction coefficient (Becker and Coppens type I with Lorentzian distribution) was 0.519(5), and the final electron density difference map was flat with a maximum of 1.24 e/Å^3 and a minimum of −1.27 e/Å^3. Refinement of the occupancy factor for the potassium atom showed that the site was fully occupied.

$Rb_2Mo_9S_{11}$ (2). The structure was refined in the trigonal space group $R\bar{3}c$ on F by full-matrix least-squares techniques with the JANA98 program. Atomic positions of $K_2Mo_9S_{11}$ were used in the first stages of the refinement of $Rb_2Mo_9S_{11}$ on the corrected data set (3755 collected reflections, 1355 unique reflections with $I/\sigma(I) > 2$, R_{int} = 0.0421). The final refinement cycle including the atomic coordinates and anisotropic displacement parameters for all atoms led to the values of $R(F_o)$ = 0.0368, $R_w(F_o)$ = 0.0379, and S = 1.76 for the independent data having $I/\sigma(I) > 2$. No twinning was observed. The maximum shift/σ ratio for the 36 refined parameters was less than 0.0008. The secondary extinction coefficient (Becker and Coppens type I with Lorentzian distribution) was 0.023(4), and the final electron density difference map was flat with a maximum of 3.03 e/Å^3 and a minimum of −3.71 e/Å^3. Refinements of the occupancy factor for the rubidium atom showed that the site was fully occupied.

$Cu_2K_{1.8}Mo_9S_{11}$ (3). As for $K_2Mo_9S_{11}$ and $Rb_2Mo_9S_{11}$, the structure was refined in the trigonal space group $R\bar{3}c$, using the JANA98 program. Atomic coordinates of $K_2Mo_9S_{11}$ were used in the first stages of the refinement on the corrected data set (3739 collected reflections, 1443 unique reflections with $I/\sigma(I) > 2$, R_{int} = 0.0273). An electron density difference map revealed two important peaks (+21 and +13

(16) Fedorov, V. E.; Elsegood, M. R. J.; Yarovoi, S. S.; Mironov, Y. V. *Chem. Commun*. **1998**, 1861.
(17) Fenske, D.; Ohmer, J.; Hachgenei, J. *Angew. Chem., Int. Ed. Engl*. **1985**, *24*, 994.
(18) Ghilardi C. A.; Midollini, S.; Saccani, L. *Chem. Commun*. **1981**, 47.
(19) Chandrasekaran, A. XRAYACS: Program for single-crystal X-ray data corrections, Massachusetts, 1998.
(20) Sheldrick, G. M. *Acta Crystallogr*. **1990**, *A46*, 467.
(21) Petricek, V. JANA98: Crystallographic Computing System for Ordinary and Modulated Structures, 1998 (JANA98 is available free of charge on the World Wide Web at: http://www-xray.fzu.cz/jana/jana98.html).
(22) Hamilton, W. C. *Acta Crystallogr*. **1965**, *18*, 502.

Table 1. X-ray Crystallographic and Experimental Data for $K_2Mo_9S_{11}$, $Rb_2Mo_9S_{11}$, $Cu_2K_{1.8}Mo_9S_{11}$, and $K_{1.8}Mo_9S_{11}$

formula	$K_2Mo_9S_{11}$	$Rb_2Mo_9S_{11}$	$Cu_2K_{1.8}Mo_9S_{11}$	$K_{1.8}Mo_9S_{11}$
formula weight	1294.3	1387.1	1413.6	1286.5
space group	$R\bar{3}c$ (no. 167)	$R\bar{3}c$ (no. 167)	$R\bar{3}c$ (no. 167)	$R\bar{3}c$ (no. 167)
a, Å	9.271(1)	9.356(2)	9.4215(4)	9.2801(8)
b, Å	9.271(1)	9.356(2)	9.4215(4)	9.2801(4)
c, Å	35.985(9)	35.935(9)	35.444(2)	35.833(7)
Z	6	6	6	6
V, Å^3	2678.6(8)	2724(1)	2724.6(2)	2672.5(6)
ρ_{calcd}, g cm^{-3}	4.813	5.073	5.169	4.798
T, °C	20	20	20	20
λ, Å	0.710 73 (Mo Kα)	0.710 73 (Mo Kα)	0.710 73 (Mo Kα)	0.710 73 (MoKα)
μ, mm^{-1}	7.829	12.566	9.932	7.8
R_1[a] ($I/\sigma(I) > 2$)	0.0186	0.0368	0.0238	0.0219
wR_2[b] ($I/\sigma(I) > 2$)	0.0207	0.0379	0.0213	0.0215

[a] $R_1 = \sum||F_o| - |F_c||/\sum|F_o|$. [b] $wR_2 = \{\sum[w(F_o - F_e)^2]/\sum[w(F_o)^2]\}^{1/2}$, $w = 1/[\sigma^2(F_o) + 0.00005F_o^2]$.

e/Å^3). On the basis of geometric considerations, the first one was attributed to a copper atom, Cu1, with a partial occupancy factor and the second one located at the origin to a supplementary potassium atom, K2, also with a partial occupancy factor. The refinement of the positional and anisotropic displacement parameters for all atoms and occupancy factor parameters for the K1, K2, and Cu1 sites led to the values of $R(F_o) = 0.0331$ and $R_w(F_o) = 0.0298$ for the 1443 independent data having $I/\sigma(I) > 2$, with two residual peaks of 4.77 and 4.57 e/Å^3, 0.4 Å from the Cu1 site and 0.5 Å from the K1 atom, respectively. At this stage of the refinement, different procedures were possible to better describe the copper and potassium distributions: addition of extra copper atoms with partial occupancy factors, delocalization of the K1 atom around the 3-fold axis, and use of anharmonic tensors.[23] The various possibilities were checked. In each case, the use of anharmonic tensors up to the fourth order led to results similar to those obtained with the split or extra-atom models. Since the anharmonic model involved more refined parameters, the harmonic ones were preferred. Then, the potassium distribution was described with a K1 atom in the general position and a K2 potassium atom at the inversion center and the copper distribution with two independent Cu1 and Cu2 atoms in the general position. The last refinement, including the atomic coordinates, anisotropic displacement parameters for all atoms, and site occupancy factors for Cu1, Cu2, K1, and K2 atoms, led to the values of $R(F_o) = 0.0238$, $R_w(F_o) = 0.0213$, and $S = 1.56$ for all independent data having $I/\sigma(I) > 2$. The obverse−reverse twinning ratio was 2.7-(2)%. The maximum shift/σ ratio for the 67 refined parameters was 0.0228, resulting from the strong correlation between Cu1 and Cu2 atoms. The secondary extinction coefficient (Becker and Coppens type I with Lorentzian distribution) was 0.137(3). The final electron density difference map was flat with a maximum of 2.07 e/Å^3 and a minimum of −1.89 e/Å^3 and without a significant residual peak around the potassium and copper sites. The stoichiometry deduced from the refinement was $Cu_{2.0(1)}K_{1.78(2)}Mo_9S_{11}$.

$K_{1.8}Mo_9S_{11}$ (4). The structure was refined in the trigonal space group $R\bar{3}c$ on F by full-matrix least-squares techniques using the JANA98 program. As the centered systematic extinctions of lattice R were not fully respected, we assumed that the crystal investigated was significantly twinned and the extinction condition was not introduced during data collection. Atomic positions of $K_2Mo_9S_{11}$ were used in the first stages of the refinement of $K_{1.8}Mo_9S_{11}$ on the data set (6106 collected reflections, 2183 unique reflections with $I/\sigma(I) > 2$; $R_{int} = 0.0175$). Due to the small-size and homogeneous shape of the crystal used, an absorption correction was not necessary ($\mu R \approx 0.2$). Refinement of the occupancy factors for all the atoms showed that the molybdenum and sulfur sites were fully occupied whereas the potassium site was occupied at 89%, leading to the $K_{1.78(1)}Mo_9S_{11}$ composition. The final refinement cycle including the atomic coordinates and anisotropic displacement parameters for all atoms led to the values of $R(F_o) = 0.0219$, $R_w(F_o) = 0.0215$, and $S = 1.96$ for the independent data having $I/\sigma(I) > 2$. The twinning ratio was 5.52(1)%. The maximum shift/σ ratio for the 38 refined parameters was less than 0.0016. The secondary extinction coefficient (Becker and Coppens type I with Lorentzian distribution) was 0.035(1), and the final electron density difference map was flat with a maximum of 1.76 e/Å^3 and minimum of −2.01 e/Å^3. No copper atom was found, in accordance with the EDS analysis, and no residual peak was observed at the origin, which is occupied by the K2 atom in $Cu_2K_{1.8}Mo_9S_{11}$.

Table 2. Atomic Coordinates and Equivalent Isotropic Displacement Parameters (Å^2) for $K_2Mo_9S_{11}$, $Rb_2Mo_9S_{11}$, $Cu_2K_{1.8}Mo_9S_{11}$, and $K_{1.8}Mo_9S_{11}$[a]

atom	site	τ	x	y	z	U_{eq}
			(**1**) $K_2Mo_9S_{11}$			
Mo1	18e	1	0	0.168 07(1)	0.25	0.006 58(4)
Mo2	36f	1	0.169 78(1)	0.159 35(1)	0.187 215(3)	0.006 92(3)
S1	18e	1	0.307 17(5)	0.307 17(5)	0.25	0.010 1(1)
S2	36f	1	0.023 95(4)	0.317 45(4)	0.192 218(8)	0.008 93(9)
S3	12c	1	0	0	0.136 03(1)	0.010 4(1)
K1	12c	1	0	0	0.053 03(1)	0.023 1(1)
			(**2**) $Rb_2Mo_9S_{11}$			
Mo1	18e	1	0	0.166 64(4)	0.25	0.005 7(1)
Mo2	36f	1	0.167 84(4)	0.158 46(4)	0.187 184(7)	0.006 26(9)
S1	18e	1	0.303 9(1)	0.303 9(1)	0.25	0.009 2(3)
S2	36f	1	0.020 7(1)	0.312 9(1)	0.191 94(2)	0.008 3(2)
S3	12c	1	0	0	0.136 23(4)	0.010 6(3)
Rb1	12c	1	0	0	0.050 81(2)	0.017 8(1)
			(**3**) $Cu_2K_{1.8}Mo_9S_{11}$			
Mo1	18e	1	0	0.166 93(3)	0.25	0.007 08(6)
Mo2	36f	1	0.163 70(2)	0.155 23(2)	0.187 703(4)	0.007 55(6)
S1	18e	1	0.303 10(8)	0.303 10(8)	0.25	0.010 6(2)
S2	36f	1	0.025 69(7)	0.317 18(7)	0.190 55(1)	0.011 5(2)
S3	12c	1	0	0	0.134 02(2)	0.012 9(2)
K1	36f	0.252(2)	0.021(2)	0.038 1(7)	0.050 18(6)	0.031(2)
K2	6b	0.265(6)	0	0	0	0.055(3)
Cu1	36f	0.19(1)	0.157 7(8)	0.266 8(6)	0.106 5(4)	0.041(2)
Cu2	36f	0.15(1)	0.224(1)	0.366(3)	0.076 9(6)	0.058(9)
			(**4**) $K_{1.8}Mo_9S_{11}$			
Mo1	18e	1	0	0.167 95(2)	0.25	0.006 59(4)
Mo2	36f	1	0.170 08(1)	0.159 46(1)	0.186 894(3)	0.007 02(3)
S1	18e	1	0.306 96(5)	0.306 96(5)	0.25	0.010 3(1)
S2	36f	1	0.024 07(4)	0.317 05(4)	0.192 236(8)	0.009 06(9)
S3	12c	1	0	0	0.135 411)	0.010 9(1)
K1	12c	0.888(2)	0	0	0.052 12(2)	0.024 8(2)

[a] U_{eq} is defined as one-third of the trace of the orthogonalized $\mathbf{U}_{ij}$ tensor. τ is the site occupancy factor.

The crystallographic and experimental data of the four compounds investigated are listed in Table 1, the atomic coordinates and equivalent isotropic displacement parameters in Table 2, and selected interatomic distances in Table 3.

Magnetic Susceptibility and Electrical Resistivity Measurements. The studies of the temperature dependences of the electrical resistivity were carried out on single crystals of $K_{1.8}Mo_9S_{11}$ (dimensions 0.46 × 0.43 × 0.18), $K_2Mo_9S_{11}$ (dimensions 0.46 × 0.35 × 0.39 mm^3), and $Cu_2K_{1.8}Mo_9S_{11}$ (dimensions 0.53 × 0.42 × 0.21 mm^3) using a conventional ac four-probe method with a current amplitude of 0.1 mA. Contacts were ultrasonicaly made with molten indium on single crystals previously characterized on a CAD-4 diffractometer. In the case of the

(23) (a) Bachman, R.; Schulz, H. *Acta Crystallogr*. **1984**, *40*, 668. (b) Zucker, U. H.; Schulz, H. *Acta Crystallogr*. **1982**, *38*, 563. (c)Kuhs, W. F. *Acta Crystallogr*. **1983**, *40*, 133.

Table 3. Selected Interatomic Distances for $K_2Mo_9S_{11}$, $Rb_2Mo_9S_{11}$, $Cu_2K_{1.8}Mo_9S_{11}$, and $K_{1.8}Mo_9S_{11}$

	$K_2Mo_9S_{11}$	$Rb_2Mo_9S_{11}$	$Cu_2K_{1.8}Mo_9S_{11}$	$K_{1.8}Mo_9S_{11}$
		Intratriangle		
Mo1−Mo1 (×2)	2.698 8(2)	2.700 3(5)	2.724 1(3)	2.699 7(2)
Mo2−Mo2 (×2)	2.646 4(1)	2.647 1(5)	2.605 0(4)	2.652 6(1)
		Intertriangle		
Mo1−Mo2	2.777 7(1)	2.772 6(3)	2.726 9(2)	2.781 2(1)
Mo1−Mo2	2.695 2(1)	2.697 5(4)	2.657 0(2)	2.697 1(1)
		Intercluster		
Mo2−Mo2	3.315 2(1)	3.363 2(3)	3.434 9(3)	3.300 8(1)
		Intratriangle		
Mo1−S1 (×2)	2.469 9(4)	2.466(1)	2.477 3(7)	2.470 6(4)
Mo2−S2	2.447 5(3)	2.450 2(9)	2.452 1(8)	2.448 1(3)
Mo2−S2	2.487 0(5)	2.478(2)	2.533(1)	2.486 1(5)
		Intertriangle		
Mo1−S2 (×2)	2.445 7(4)	2.449(1)	2.481 9(6)	2.437 1(4)
Mo2−S1 (×2)	2.619 1(3)	2.614 5(6)	2.590 7(3)	2.619 5(3)
Mo2−S3 (×2)	2.393 2(3)	2.385(1)	2.425 3(8)	2.397 7(3)
		Intercluster		
Mo2−S2	2.492 9(4)	2.501(1)	2.523 0(5)	2.483 3(4)
M1−S1 (M = K,Rb)	3.398 2(3) (×3)	3.468(1) (×3)	3.27(2)	3.411 3(3) (×3)
M1−S1			3.47(2)	
M1−S1			3.77(1)	
M1−S2	3.225 0(5) (×3)	3.267(1) (×3)	3.01(1)	3.218 2(5) (×3)
M1−S2			3.25(1)	
M1−S2			3.520(8)	
M1−S3	2.986 8(8)	3.069(2)	2.988(3)	2.984 5(8)
M1−M1	3.817(1)	3.651 6(9)	3.611(3)	3.735(1)
K1−K1			0.54(1)	
K2−S2 (×6)			3.227 3(8)	
K2−K1 (×6)			1.806(5)	
Cu1−S1			2.305(9)	
Cu1−S2			2.20(1)	
Cu1−S3			2.396(7)	
Cu1−Cu1			1.97(2)	
Cu1−Cu2			0.67(2)	
Cu2−Cu2			0.70(3)	
Cu2−S1			2.27(1)	
Cu2−S2			2.43(2)	
Cu2−S2			2.75(2)	

$Cu_2K_{1.8}Mo_9S_{11}$ compounds, the cell parameters, depending on the quantity of copper inserted, were found identical in the crystal used for the structural determination and that used for electrical measurements, both coming from the same preparation. The ohmic behavior and the invariance of the phase were checked during the different measurements at low and room temperature.

Magnetic susceptibility measurements were carried out using an SHE-906 SQUID susceptometer from 20 to 2 K on a cold-pressed pellet (ca. 100 mg) of $K_{1.8}Mo_9S_{11}$.

Extended Hückel Calculations. Extended Hückel molecular[24] and tight-binding[25] calculations were carried out using the programs CACAO[26] and YaEHMOP,[27] respectively. The experimental data of the crystal structure of $K_2Mo_9S_{11}$ were used. The exponents (ζ) and the valence shell ionization potentials (H_{ii}, eV) were respectively 1.817 and −20.0 for S 3s, 1.817 and −13.3 for S 3p, 1.956 and −8.34 for Mo 5s, 1.921 and −5.24 for Mo 5p, 0.874 and −4.34 for K 4s, and 0.874 and −2.73 for K 4p. H_{ii} values for Mo 4d were set equal to −10.50. A linear combination of two Slater-type orbitals of exponents $\zeta_1 = 4.542$ and $\zeta_2 = 1.901$ with the weighting coefficients $c_1 = c_2 = 0.6097$ was used to represent the Mo 4d atomic orbitals. The density of states of $K_2Mo_9S_{11}$ was obtained using a set of eight k points.

Results and Discussion

Structure of $K_2Mo_9S_{11}$ (1) and $Rb_2Mo_9S_{11}$ (2). $K_2Mo_9S_{11}$ was first thought to be isostructural with the $Tl_2Mo_9S_{11}$ compound (SG $R\bar{3}$, $a = 9.304(3)$ Å, $c = 35.366(7)$ Å) which contains an equal mixture of Mo_6S_8 and $Mo_{12}S_{14}$ units.[28] Single-crystal X-ray diffraction studies have revealed in turn that $K_2Mo_9S_{11}$ and $Rb_2Mo_9S_{11}$ (SG $R\bar{3}c$, $a = 9.271(1)$ Å, $c = 35.985(9)$ Å and $a = 9.356(2)$ Å, $c = 35.935(9)$ Å, respectively) crystallize in a new structural type, the three-dimensional framework of which is only based on interconnected Mo_9S_{11} clusters. The Mo_9S_{11} unit (Figure 1) can be classically described as the result of the uniaxial face-sharing condensation of two Mo_6S_8 units with loss of S atoms belonging to the shared face. Such a unit can also be seen as the stacking of three planar Mo_3S_3 units, instead of two in Mo_6S_8, with two supplementary chalcogen atoms capping the outer triangular faces. The median plane Mo_3S_3 contains three 2-fold axes which are perpendicular to the 3-fold axis, and therefore, the Mo_9S_{11} unit has point symmetry D_3. The projection of the arrangement of the Mo_9S_{11} units onto the hexagonal plane (110) is illustrated for $K_2Mo_9S_{11}$ in Figure 2. Each unit is centered on a 6a position (0,0,1/4) and is connected to six adjacent units via twelve interunit Mo2−S2

(24) Hoffmann, R. *J. Chem. Phys*. **1963**, *39*, 1397.
(25) Whangbo, M.-H.; Hoffmann, R. *J. Am. Chem. Soc*. **1978**, *100*, 6093.
(26) Mealli, C.; Proserpio, D. *J. Chem. Educ*. **1990**, *67*, 399.
(27) Landrum, G. A. YAeHMOP—Yet Another extended Huckel Molecular Orbital Package, version 2.0, Ithaca, NY, 1997 (YAeHMOP is available free of charge on the World Wide Web at http://overlap.chem.cornell.edu:8080/yaehmop.html).
(28) (a) Potel, M.; Chevrel, R.; Sergent, M.; Decroux, M.; Fischer, Ø. *C. R. Acad. Sci. Paris* **1979**, *288C*, 429. (b) Chevrel, R.; Potel, M.; Sergent, M.; Decroux, M.; Fischer, Ø. *J. Solid State Chem*. **1980**, *34*, 247. (c) Potel, M.; Chevrel, R.; Sergent, M. *Acta Crystallogr*. **1980**, *B36*, 1319.

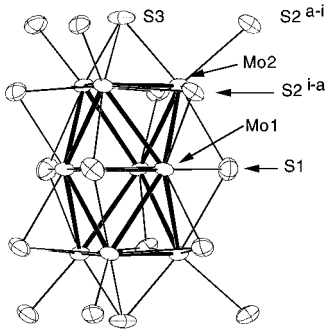

Figure 1. $Mo_9S_5{}^iS_{6/2}{}^{i-a}S_{6/2}{}^{a-i}$ cluster unit (97% probability ellipsoids).

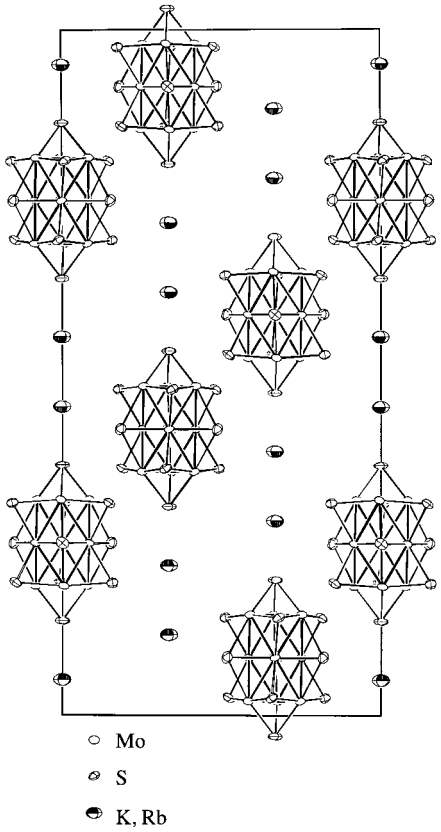

Figure 2. Arrangement of the Mo_9S_{11} units and alkaline cations on the [110] plane in the $M_2Mo_9S_{11}$ (M = Rb, K) structure (intercluster distances have been omitted for clarity) (97% probability ellipsoids).

bonds (**1**, Mo−S = 2.493 Å; **2**, Mo−S = 2.501 Å), to form a three-dimensional Mo−S framework, the connective formula of which is $[Mo_9S_5{}^iS_{6/2}{}^{i-a}]S_{6/2}{}^{a-i}$ in Schäfer's notation.[29] It results from this arrangement that the shortest intercluster Mo2−Mo2 distances are 3.31 and 3.36 Å for the K and Rb compounds, respectively. The increase of the intercluster distances results from the larger ionic radius of Rb with respect to that of K.

The inner Mo1 and outer Mo2 atoms do not have the same environment. Mo2 atoms of the outer Mo_3 triangles have an environment similar to that encountered in the Mo_6S_8 units of the rhombohedral MMo_6X_8 (M = Na, Pb, RE, ...) (X = S, Se) compounds.[3] They are surrounded by four Mo atoms (two inner Mo1 atoms and two outer Mo2 atoms) and four S atoms, which are approximately coplanar, and another S atom belonging to an adjacent Mo_9S_{11} cluster and constituting the apex of a square-based pyramidal environment. Mo1 atoms of the inner Mo_3 triangle are surrounded by six Mo atoms (2 inner Mo1 atoms and 2 × 2 outer Mo2 atoms) and only four S atoms belonging to the same cluster unit.

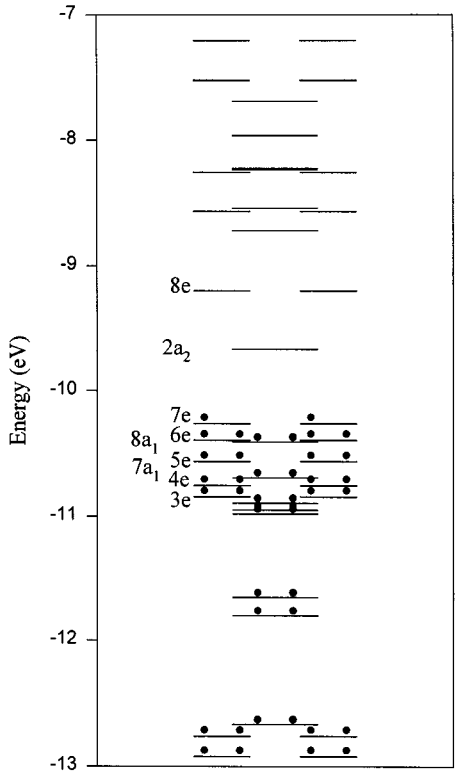

Figure 3. Molecular orbital diagram of the $[Mo_9S_{11}]^{2-}$ unit of D_3 symmetry.

As observed in previous molybdenum condensed cluster chalcogenides,[9] two kinds of Mo−Mo distances can be distinguished in the units: the Mo−Mo intratriangle distances ranging from 2.647 to 2.699 Å and the Mo−Mo intertriangle ones ranging from 2.695 to 2.778 Å. The Mo−S bond distances are typical, with the shortest ones at 2.393 and 2.385 Å for Mo2−S3 in **1** and **2**, respectively, and the longest ones at 2.619 and 2.615 Å for Mo2−S1 in **1** and **2**. It is worth mentioning that the overall sets of distances in the Mo_9S_{11} clusters are very similar in the Rb and K analogues. The largest difference is less than 0.3%, which indicates that the Mo_9S_{11} clusters formally bear the same negative formal charge, namely, 2−. The alkali-metal cations are well-ordered and located along the 3-fold axes between the Mo_9S_{11} units, leading to a stacking sequence of −M−Mo_9S_{11}−M−. Each cation is seven-coordinated with six S atoms (three S1 atoms and three S2 atoms: 3.398 Å and 3.225 Å in **1**, 3.468 Å and 3.267 Å in **2**), forming an octahedron compressed along the 3-fold axis, and the seventh, an S3 terminal atom, capping one face of the octahedron (2.987 Å in **1**, 3.069 Å in **2**).

Electronic Structure of $K_2Mo_9S_{11}$. Extended Hückel molecular and tight-binding calculations were performed on the isolated $[Mo_9S_{11}]^{2-}$ and the three-dimensional $K_2Mo_9S_{11}$ structure, respectively. The electronic structure of Mo_9X_{11} (X = S, Se) has been studied previously.[30,31] The energy diagram of $[Mo_9S_{11}]^{2-}$ with D_3 symmetry is recalled in Figure 3 for the sake of understanding. As noted previously for this kind of material, the overall distribution of energy levels shows a rough separation of the chalcogen p and molybdenum d states with a predominant metallic character in the HOMO/LUMO region

(29) Schäfer, H.; Von Schnering, H. G. *Angew. Chem.* **1964**, *20*, 833.
(30) Hughbanks, T.; Hoffmann, R. *J. Am. Chem. Soc.* **1983**, *105*, 3528.
(31) Gautier, R.; Gougeon, P.; Halet, J.-F.; Potel, M.; Saillard, J.-Y. *J. Alloys Compds.* **1997**, 311.

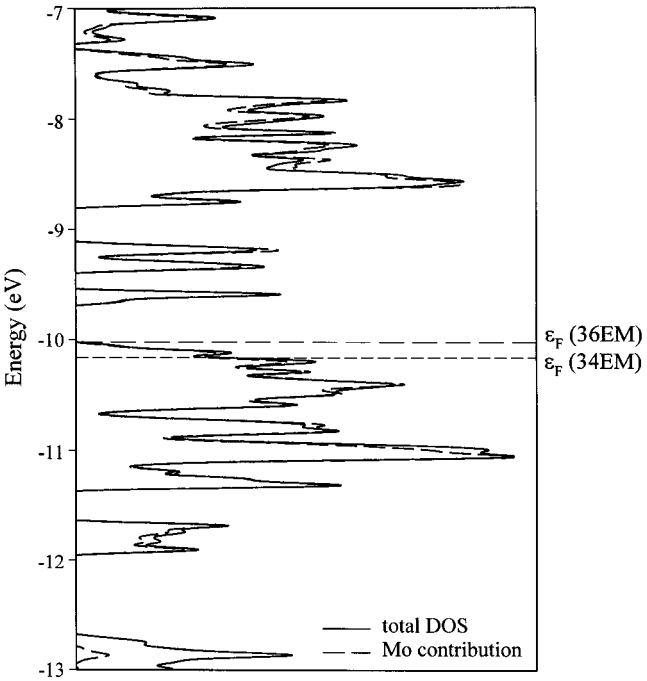

Figure 4. Total density of states (solid line) and metal contribution of $K_2Mo_9S_{11}$.

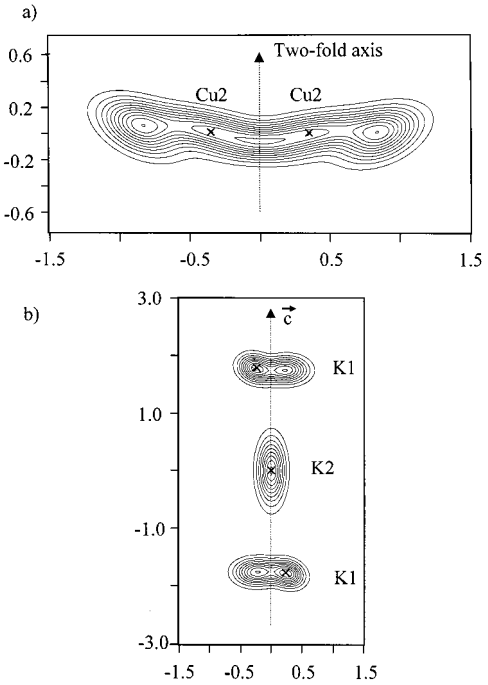

Figure 5. Joint probability density function (pdf) maps for (a) Cu1 and Cu2 in the plane defined by Cu2 and the 2-fold axis (Cu1 atoms, situated at a maximum of probability density, are on both sides of the plane and thus are not shown (min/max 0/4422 $Å^{-3}$, step 400 $Å^{-3}$)) and (b) K1 and K2 in the *ac* plane (K^+ cations are indicated by +; K1 atoms are delocalized around the 3-fold axis (min/max 0/7441 $Å^{-3}$, step 750 $Å^{-3}$)).

and the existence of a large energy gap separating the bonding and antibonding Mo d-based molecular orbitals.

An open-shell electronic configuration is found for the $[Mo_9S_{11}]^{2-}$ oligomer, that is, for 34 MEs with the 7e HOMO partially filled. Being Mo−Mo nonbonding overall, addition of extra electrons in this 7e MO predominantly localized on the outer Mo2 atoms should be possible without altering the structural arrangement much and leading to a closed-shell electron configuration. A large HOMO−LUMO gap separating the 7e MO from the antibonding $2a_2$ MO would then be observed for the count of 36 MEs, corresponding formally to a $[Mo_9S_{11}]^{4-}$ unit.

EHTB calculations carried out on the 3-D $K_2Mo_9S_{11}$ solid material confirm these assumptions. Around the Fermi level, the density of states shown in Figure 4 is made of rather narrow bands, which derive from MOs of the HOMO/LUMO region of the "molecular" Mo_9S_{11} units. The Fermi level at −10.18 eV crosses a partially filled band which mainly comes from the 6e and 7e MO levels. Owing to the weakly bonding character of the Mo−Mo intercluster separation of 3.31 Å (the intercluster Mo−Mo overlap population is significantly positive (0.04)), $K_2Mo_9S_{11}$ should be metallic as confirmed experimentally (vide infra).

If two extra electrons per Mo_9S_{11} are added to give a unit that is $[Mo_9S_{11}]$,$^{4-}$ this band becomes completely filled, with the Fermi level lying at −10.04 eV. Such an electron count would render this material semiconducting through suitable doping. Indeed, Mo−Mo and Mo−S overlap populations hardly change overall upon addition of electrons. A comparison of these overlap populations for $[Mo_9S_{11}]^{2-}$ and $[Mo_9S_{11}]^{4-}$ indicates that the intercluster Mo2−Mo2 and intracluster Mo1−Mo1 distances should slightly lengthen, as well as Mo−S distances, whereas the intracluster Mo2−Mo2 distances should slightly shorten when electrons are added.

Structure of $Cu_2K_{1.8}Mo_9S_{11}$. To give further support to the theoretical results, attempts to increase experimentally the number of electrons per Mo_9S_{11} cluster in $K_2Mo_9S_{11}$ were performed. Several possibilities were envisaged: partial replacement of the molybdenum by a more electron-rich 4d or 5d element such as Ru or Re, substitution of a divalent cation (Ba^{2+}, Pb^{2+}) for K^+, or insertion of a small reducing transition-metal element into the small-size crystallographic voids. The last procedure was chosen, by insertion of copper into the structure. This led to the new metastable quaternary compound of formula $Cu_2K_{1.8}Mo_9S_{11}$ (SG $R\bar{3}c$, a = 9.4215(4) Å, c = 35.444(2) Å) in which the structural arrangement of the Mo_9S_{11} units is maintained. In $Cu_2K_{1.8}Mo_9S_{11}$, the metal−metal distances vary as expected from the theoretical calculations (Table 2). Thus, the Mo2−Mo2 (outer) intratriangle bond lengths decrease slightly, whereas the Mo1−Mo1 (inner) ones increase slightly (less than 2%). Moreover, no significant modification of the intertriangle distances is noticed. The most important change concerns the intercluster distances which lengthen from 3.3152(1) to 3.4348(2) Å in the quaternary phase.

The potassium distribution is mainly described by the K1 atom in the general position, delocalized around the potassium site occupied in $K_2Mo_9S_{11}$, and by the K2 atom, at the origin (Figure 5). Both sites are partially occupied. The K1 atom is surrounded by seven sulfur atoms, forming a monocapped octahedron. The K2 atom is coordinated to six sulfur atoms forming an octahedron in which one face is common to the K1 environment (Figure 6). K1 and K2 sites are 1.806 Å apart and, thus, cannot be occupied simultaneously.

The copper distribution can be modeled by two atoms in the general position with partial occupancy factors in sites which are 0.67 Å apart (Figures 5 and 6). Both of them are in triangular coordination with sulfur with Cu−S distances ranging from 2.20 to 2.94 Å. The delocalization of the potassium atom probably results from the small Cu−K distance (K1−Cu1 = 2.74 Å, K1−Cu2 = 2.59 Å), compared to those commonly found in the

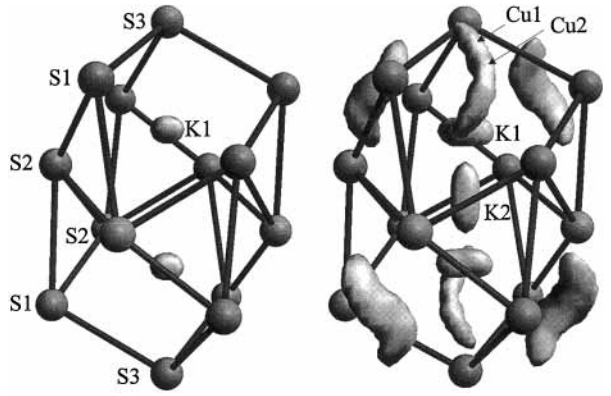

Figure 6. On the left, 3D surface plots of the pdf of K1 with their sulfur environment in $K_2Mo_9S_{11}$ and, on the right, 3D surface plot of the jpdf of Cu1, Cu2, K1, and K2 with the sulfur environment of potassium in $Cu_2K_{1.8}Mo_9S_{11}$. The Cu^+ cations influence the potassium position, leading to its delocalization on K1 and K2 sites. The Cu jpdf of "twisted cocoon"-like shape includes two Cu1 and two Cu2 atoms. A 2-fold axis goes through the center of this jpdf (isosurface at 95% of density probability for K, and Cu).

literature (ca. 3.50 Å).[32] Such small distances must involve strong electrostatic repulsion between the K^+ and Cu^+ ions that could be responsible for the partial deinsertion of the potassium atoms (10%).

Structure of $K_{1.8}Mo_9S_{11}$. The potassium nonstoichiometry in $Cu_2K_{1.8}Mo_9S_{11}$ was confirmed by the deintercalation of the copper that leads to the $K_{1.78(1)}Mo_9S_{11}$ composition (SG $R\bar{3}c$; a = 9.2801(8) Å, c = 35.833(7) Å). In this structure, the three-dimensional Mo−S framework is maintained. The Mo−Mo distances are, overall, very close to those observed in $K_2Mo_9S_{11}$, with the largest difference being smaller than 1% (Mo−Mo distances range from 2.653 to 2.782 Å). Similarly, Mo−S bonds differ by less than 0.4%, ranging from 2.398 to 2.619 Å. The potassium atoms occupy the same special position on the 3-fold axis as in $K_2Mo_9S_{11}$ and thus are surrounded by seven sulfur atoms, forming a distorted monocapped octahedron (K−S separations range from 2.98 to 3.41 Å). The site at the origin, occupied by the K2 atom in $Cu_2K_{1.8}Mo_9S_{11}$, is empty in $K_{1.8}Mo_9S_{11}$. It is noteworthy to mention that the removal of copper leads to the relocalization of the potassium atom back into its initial site. This confirms the Cu^+−K^+ electrostatic repulsion in the quaternary phase.

Resistivity Properties. Variable-temperature resistivity data for single crystals of $K_2Mo_9S_{11}$ and $Cu_2K_{1.8}Mo_9S_{11}$ in the temperature range 4−290 K are presented in Figure 7. $K_2Mo_9S_{11}$ exhibits poor metallic behavior with a room temperature (RT) resistivity of 5×10^{-4} Ω·cm. The temperature dependence of the resistivity indicates an unusual behavior, with the $\rho_{(T)}/\rho_{RT}$ ratio decreasing from 1 at 290 K to 0.7 at 110 K, then increasing from 0.7 to 1.4 down to 30 K, and finally decreasing again. Resistivity measurements carried out on several $K_2Mo_9S_{11}$ single crystals confirm this unusual behavior and show that this compound is near a metal−insulator boundary. Previous works on other condensed molybdenum cluster chalcogenides led to similar conclusions.[5b,33]

As expected from theoretical calculations, addition of extra electrons changes the electrical properties. Thus, the compound $Cu_2K_{1.8}Mo_9S_{11}$, in which the number of MEs is 35.8, very close to the closed-shell configuration of 36, becomes semiconducting with a resistivity of 2.5×10^{-3} Ω·cm at room temperature and

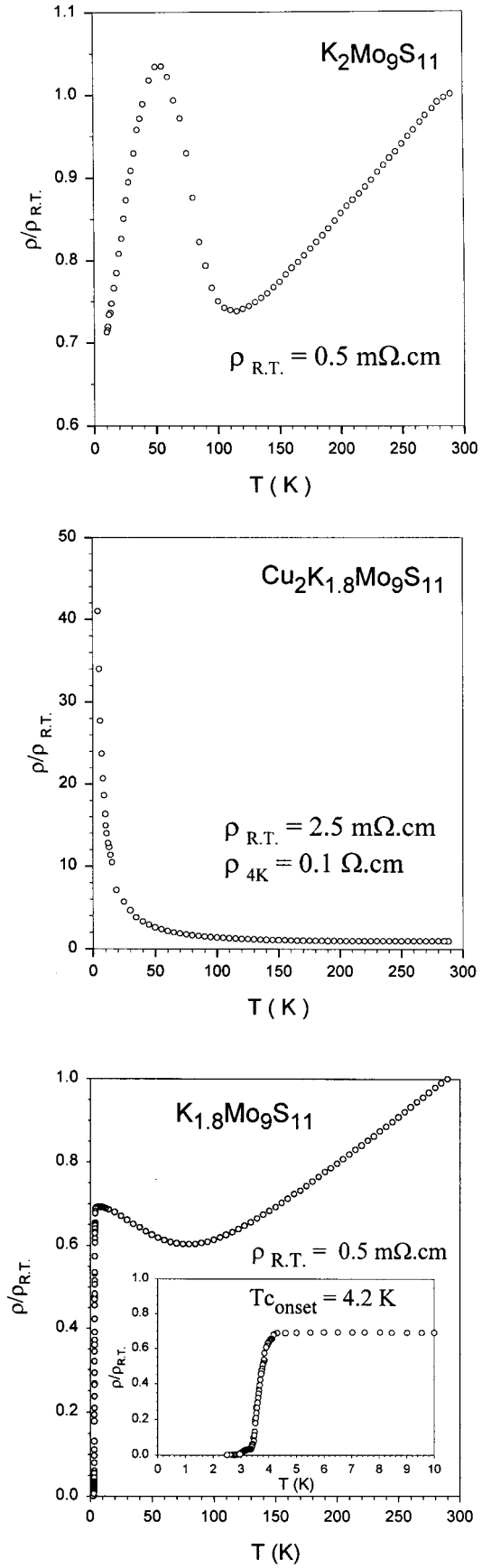

Figure 7. Temperature dependences of the resistivities of $K_2Mo_9S_{11}$, $Cu_2K_{1.8}Mo_9S_{11}$, and $K_{1.8}Mo_9S_{11}$ single crystals.

(32) ICSD, Inorganic Crystal Structure Database, Gmelin−Institut für Anorganische Chemie und Fachinformationszentrum, FIZ Karlsruhe, 1995.

(33) Brusetti, R.; Laborde, O.; Sulpice, A.; Calemczuk, R.; Potel, M.; Gougeon P. *Phys. Rev. B* **1995**, *52*, 4481.

0.1 Ω·cm at 4 K. On the other hand, the copper deintercalated compound $K_{1.8}Mo_9S_{11}$ shows a metallic behavior with a superconducting transition occurring at 4.2 K (Figure 7), contrary to $K_2Mo_9S_{11}$ which remains metallic at least above 2 K. This was also confirmed by magnetic susceptibility measurements, carried out on a cold-pressed pellet of $K_{1.8}Mo_9S_{11}$, which indicate a superconducting behavior below 4.5 K. Supplementary experiments are in progress to increase the potassium deficiency and then to follow the electrical properties versus the number of MEs.

Conclusion

The series of the four new compounds $M_2Mo_9S_{11}$ (M = K, Rb), $Cu_2K_{1.8}Mo_9S_{11}$, and $K_{1.8}Mo_9S_{11}$ were synthesized. Single-crystal X-ray diffraction studies showed that their structures contain, for the first time, quasi-isolated Mo_9S_{11} units forming an original three-dimensional network. The crystal structure of $M_2Mo_9S_{11}$ is particularly adapted for the insertion of small cations such as Cu^+, since copper could be inserted at the cost of a small K^+ loss, leading to $Cu_2K_{1.8}Mo_9S_{11}$. In accordance with theoretical studies, the resistivity behavior of the title compounds was found to strongly depend on the number of metallic electrons per Mo_9S_{11} motif. Thus, $K_2Mo_9S_{11}$ which contains 34 MEs is metallic, whereas $Cu_2K_{1.8}Mo_9S_{11}$ is semiconducting with 35.8 MEs. In addition, the deintercalation of Cu ions yields the superconducting compound $K_{1.8}Mo_9S_{11}$ with 33.8 MEs (T_c = 4.5 K).

Acknowledgment. Thanks are expressed to Pr. J.-Y. Le Marouille for the use of the Silicon Graphic Station and Pr. J.-Y. Saillard for helpful comments. 3-D surface plots of the pdf were made using the SciAn program (Supercomputer Computations Research Institute, Florida State University, Tallahassee, FL).

Supporting Information Available: X-ray crystallographic files in CIF format. This material is available free of charge via the Internet at http://pubs.acs.org.

IC990362B